

Simultaneous in Vitro and in Vivo Validation of Nitrogen-13-Ammonia for the Assessment of Regional Myocardial Blood Flow

C. Riccardo Bellina, Oberdan Parodi, Paolo Camici, Piero A. Salvadori, Luigi Taddei, Lucio Fusani, Riccardo Guzzardi, Gerald A. Klassen*, Antonio L'Abbate, and Luigi Donato

C.N.R. Institute of Clinical Physiology and Istituto di Patologia Medica I, University of Pisa, Pisa, Italy

Measurement of myocardial blood flow by $^{13}\text{NH}_3$ relies heavily on the assessment of both the input function and the variable tissue extraction fraction. In six open-chest dogs, myocardial and arterial $^{13}\text{NH}_3$ activity was measured both by in vitro sampling and by in vivo positron emission tomography (PET). Regional myocardial blood flow was forced to vary in the range 0.2-5 ml/min/g and actual values were assessed by in vitro counting of ^{153}Gd microspheres. The ammonia input function was processed by: (a) total curve integration; (b) curve integration for 2 min; (c) integral of a fitted curve (gamma variate in vivo and exponential of the downslope in vitro). Method C brought to regional flow values which best approximated microspheres data. The in vitro correlation allows for correcting in vivo values for the flow-dependent extraction fraction. The method can be easily applied for regional myocardial blood flow measurements with PET in human studies.

J Nucl Med 1990; 31:1335-1343

A quantitative, noninvasive measurement of regional myocardial blood flow (RMBF) still remains one of the major goals in clinical cardiology.

The introduction of positron emission tomography (PET) has made possible the measurement of regional concentrations of positron emitting radiopharmaceuticals in heart muscle as well as in most organs with high accuracy (1). Different tracers have been proposed for the noninvasive assessment of RMBF in man by means of PET. Nitrogen-13-ammonia ($^{13}\text{NH}_3$) has been carefully investigated, and seems to possess several advantages that could be exploited for RMBF with PET (2-5).

Shah et al. (6) reported a good correlation between radioactive microspheres and $^{13}\text{NH}_3$ in measurement of

RMBF in dogs, although a systematic underestimation was observed by in vivo measurements. Nitrogen-13-ammonia, like all liquid deposit flow tracers, is extracted from blood with an extraction fraction <100% and is then trapped metabolically in tissue (2,4). Both factors raise the question about whether the $^{13}\text{NH}_3$ effectively retained in myocardium (net extraction fraction) may depend on factors other than blood flow alone (7,8).

Another aspect to consider is whether ^{13}N activity in blood is all due to ammonia or also to the early appearance of ^{13}N -amino acids (2,7,9) and ^{13}N -urea (9) in plasma. Labeled metabolites may affect the accuracy in determining the input function and, eventually, contaminate myocardial tracer activity recorded externally by PET. For this reason, a dynamic description of the primary curve, rather than an empirical termination 2 min following tracer injection (6), might provide a more correct quantitation of RMBF.

The newer generation of PET cameras offers higher temporal resolution that allows one to perform faster dynamic studies (10). In view of the superior performance, a better temporal definition of the tracer's input function is theoretically feasible.

The purpose of the present study was to re-examine the accuracy of $^{13}\text{NH}_3$ and PET in the measurement of RMBF. This was achieved in open-chest anesthetized dogs by:

1. In vitro measurements of ^{13}N content in serial blood samples and tissue specimens to assess arterial input function and correlate $^{13}\text{NH}_3$ flow with microsphere flow, respectively.
2. Definition of a new algorithm for input function calculation and comparison with previously proposed methods.
3. Validation of the input function obtained by dynamic PET acquisitions versus that assessed by in vitro counting.
4. Measurement of RMBF by PET and correlation with microsphere flow.

Received Sept. 14, 1989; revision accepted Mar. 19, 1990.
For reprints contact: Dr. C.R. Bellina, CNR Institute of Clinical Physiology, via Savi 8, 56100 Pisa, Italy.
* Present address: Dalhousie University, Department of Medicine, Nova Scotia, Canada.

The results derived from in vitro measurements, compared with those obtained by dynamic PET in the same animals, permitted a step-by-step analysis of potentials and problems in the evaluation of myocardial perfusion by $^{13}\text{NH}_3$ and PET.

MATERIALS AND METHODS

Animal Preparation

Studies were performed in 6 mongrel dogs weighing from 12 to 33 kg. The animals were anesthetized with thiopental sodium (30 mg/kg i.v.), intubated, and ventilated with room air enriched with oxygen. Anesthesia was maintained with intravenous (i.v.) alpha-chloralose (30 mg/kg loading dose followed by 10 mg/kg/hr). Samples for arterial blood gases content were taken at different times. Two polyethylene catheters were placed in the descending aorta for blood sampling (microspheres and ammonia) and pressure recording and in the inferior vena cava for $^{13}\text{NH}_3$ injection. Lead II of the electrocardiogram was continuously monitored. A left thoracotomy was performed and the heart suspended in a pericardial cradle. A polyethylene cannula was placed in the left atrium via the left atrial appendage for microsphere injection. The dog was positioned on the bed of our ECAT III Positron Tomograph (CTI Inc., Knoxville, TN) in order to have the center of gravity of the left ventricle as close as possible to the center of both the axial and transaxial fields of view. In addition, the gantry of the tomograph was tilted and rotated to be perpendicular to the long axis of the left ventricle. The interplane lead septum was inserted and the collimator opening was set to 36 mm, thus having an axial resolution of ~10 mm, in terms of full width at half maximum (FWHM), in the center of the field of view for each plane.

Study Protocol

Before performing the emission study, a circular ring source filled with ~4.5 mCi of gallium-68 (^{68}Ga) was used for the blank and transmission data acquisition in order to measure the attenuation correction coefficients to be used for each line of response of the sinogram. After removing the ring source, a bolus of 10-15 mCi of $^{13}\text{NH}_3$, produced according to previously described methods (11), contained in 10 ml of saline, was injected over a 10-sec period into the inferior vena cava, while carbonized polystyrene gamma-emitting microspheres ($15 \pm 1 \mu\text{m}$) labeled with gadolinium-153 (^{153}Gd) (gamma rays energy: 103 keV) were simultaneously injected into the left atrium. A timed arterial withdrawal from the femoral artery served as the reference sample for myocardial blood flow measurement with microspheres (12). The in vitro input function for $^{13}\text{NH}_3$ was determined by withdrawing serial arterial blood samples (2 ml every 10 sec for the initial 210 sec, one sample at 240 sec and then every 60 sec over an 11-min period, for a total of 14 min). PET data acquisition started at the beginning of ammonia injection. A total of 45 ungated emission tomograms were acquired in 14 min (40 frames, each of 6 sec, from 0 to 240 sec, and 5 frames, each of 120 sec, from 240 to 840 sec). The different timing between PET and in vitro blood data acquisition was due to the intrinsic limitations imposed by manual sampling. Obviously, a higher number of points would allow a better definition of the initial portion of the arterial input function.

Two experiments were performed during control hemodynamic condition. In two dogs, myocardial flow was increased by i.v. dipyridamole (0.56 mg/Kg over 4 min). In two dogs, the left anterior descending coronary artery was dissected free from surrounding tissue at ~2-3 cm from its origin and an occluder device was placed around the vessel in order to produce regional myocardial ischemia. Tracer injection and blood sampling was started 4 min after completion of dipyridamole infusion in the hyperemic experiments, 20 min after coronary occlusion in the low flow experiments and after 30 min equilibration following instrumentation of the animals in all cases. In order to attain an almost steady-state of hemodynamics and perfusion during the study, we did not address our evaluation to other clinically important conditions such as prolonged severe ischemia and reperfusion. At the end of the experiment, cardiac arrest was induced by i.v. concentrated KCl and the heart was removed rapidly.

Two to three midventricular slices of ~1 cm thickness that corresponded approximately to the tomographic image plane (marked on the animal's heart and matched to the laser source of the tomograph in line with the detectors) were sectioned orthogonally to the long axis of the left ventricle. Sixteen tissue wedges (epi-endocardial wedges) were obtained from each myocardial slice.

Blood and tissue samples were weighed on an analytical balance and counted in a NaI (TI) well counter to determine ^{13}N activity. The next day, after complete decay of ^{13}N , the tissue samples were counted again to assess microsphere concentration.

In Vitro Data Analysis

The well counter was connected to a personal computer through a dedicated interface. Vial number, time elapsed from the beginning of tracer injection, counts, and counting time were recorded for each sample.

Counting time was chosen in order to have a minimal statistics of 10k cts. Both tissue and blood data were corrected to obtain normalized cps/g (C), as follows:

$$C = \frac{C_a \cdot k \cdot vc \cdot dtc}{(e^{-kt_t} - e^{-k(t_t + t)}) \cdot W}$$

where C_a are the acquired counts (cts), k is the ^{13}N decay constant (sec^{-1}), t_t is the time when sample counting was started (sec elapsed from ammonia injection), t is the total counting time (sec), W is the weight of the sample (g), vc is a calibration factor of the well counter efficiency as a function of W , and dtc is the dead time correction factor for the well counter as a function of C_a/t .

The blood-activity curve was log transformed to find the best linear fit on the initial part of the downslope portion, i.e., the first exponential on the linear scale.

RMBF times $^{13}\text{NH}_3$ extraction (RMBFe) was calculated according to the equation:

$$\text{RMBFe} = \frac{C_m \cdot 60}{\int_0^T C_b(t) dt \cdot G_b} \quad (\text{ml/min/g}),$$

where C_m and $C_b(t)$ are ^{13}N activity concentrations (cps/g) in the myocardium and blood at time t , respectively, and G_b is the gravity of blood (1.05 g/ml). RMBF assessed by micro-

spheres was calculated using the arterial reference sample technique (12).

Three different methods were used for computing the integral of the input function: (a) $T = 14$ min (total observation time); (b) $T = 2$ min, according to Shah et al. (6); (c) $T = \infty$, while $C_b(t)$ is fitted and extrapolated on the first exponential, as described above (i.e., the first-pass portion is extracted).

Integrals of the curves were evaluated using the trapezoidal approximation method.

PET Data Analysis

The sinograms were normalized according to the tomograph nonuniformity map, corrected for attenuation, and then reconstructed using a Hanning filter with a cutoff of 0.5, thus, having a transaxial spatial resolution of ~ 9 mm FWHM. The sum of the rates of randoms and multiples related to each sinogram was used for deadtime loss correction (13). Sinograms corresponding to the bolus transit through the left ventricle were added together and the resultant image was used for detecting the inner left ventricular contour. Data were displayed as images within a 256×256 matrix of pixels. A small region of interest (ROI) was drawn within the left ventricular cavity in order to minimize spillover from the wall and avoid underestimation of the count density. Size and shape of the ROI were assessed on the last equilibrium image. The time-activity curve was computed inside the ROI and data values were then corrected for decay and deadtime losses. The better temporal resolution of the in vivo arterial data obtained with PET allowed to fit the initial portion of the curve with a gamma variate (14), and the derived integral was expressed as counts/voxel.

In order to attain an automatic edge detection of the left ventricular wall and calculate the tissue activity from the last 120-sec PET image, a dedicated computer program was developed. The major steps of the procedure are as follows:

- A. The operator manually defines two circular ROIs, one for the determination of both the center of the left ventricular cavity and the size of the computation area and the other to cut off the right ventricle.
- B. A logical product is performed between the two ROIs and only the resultant area is used for further computations.
- C. Taking the center of rotation as defined in A, the area is divided counterclockwise in 72 wedges of 5° each.
- D. Each wedge is divided in sectors (one pixel thick) from the center to the periphery and an activity profile is extracted (Fig. 1); activity values are corrected for decay and deadtime losses and then averaged in cts/sec/voxel.
- E. The peak activity of each profile and the overall maximal activity of the 72 profiles are determined; then the operator sets a threshold as percent of the maximal activity.
- F. The peak activity point for each profile is found. If the activity is greater than the selected threshold, the region corresponding to the ventricular wall is determined including all points ranging from 50% of peak activity on one side to 50% on the other (Fig. 1). If the peak activity is less than the threshold (e.g., ischemic region), the range of points is extracted from the previous wedge; the average wall activity of the wedge is thus determined.
- G. The mean wall thickness of each wedge is computed

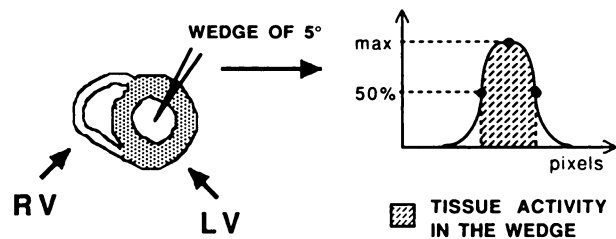


FIGURE 1

Graphical representation of how tissue activity in the PET image is automatically evaluated for each of the 72 wedges. The plot on the right shows the activity curve obtained, as a virtual profile, from the center to the periphery of the left ventricular cavity. LV = left ventricle; RV = right ventricle; max = peak activity.

multiplying the pixel size by the number of points used in step E. The wall activity is divided by a recovery coefficient as a function of the thickness to correct for partial volume effect (the measured thickness was in all cases >9 mm, i.e., the minimum detectable). The recovery function was previously determined running the program, with no correction algorithm, for determining the activity concentration in a circular eccentric heart phantom developed for the assessment of the physical performance of the tomograph (13).

- H. The wall activity is averaged packing (9 by 9) the 72 wedges in the final 8 wedges corresponding to those used for the in vitro measurements. Even if the spatial resolution of the tomograph employed in this study is much improved relative to cameras of the previous generation, it is still inadequate to explore transmural flow distribution across the myocardial wall. Thus, sub-epicardial and subendocardial in vitro data were averaged to give transmural values comparable with the PET information. For the comparison between in vitro measurements and in vivo PET data, the ventricular slice which best correlated with the anatomical details of the tomographic plane was chosen. Thus, in the six dogs, 48 ROIs were compared with the corresponding 48 tissue wedges.
- I. RMBFe values assessed by PET are computed for the eight wedges dividing the wall activity (cts/min/voxel) by the integral (cts/voxel) of the PET input function. The final result is expressed as voxel/min/voxel or ml/min/ml and can be converted to ml/min/g dividing by tissue gravity (1.08 g/ml).

RESULTS

In all dogs, the hemodynamic parameters and blood gases did not change $\pm 5\%$ in between tracer injection and KCl-induced heart arrest.

The in vitro tissue distribution of ^{13}N activity correlated well with the microsphere distribution, both expressed as percent of maximal tissue activity (Fig. 2). Furthermore, a significant linear correlation was found between the myocardial $^{13}\text{NH}_3$ concentration measured in vitro and that assessed in vivo with PET ($r = 0.94$,

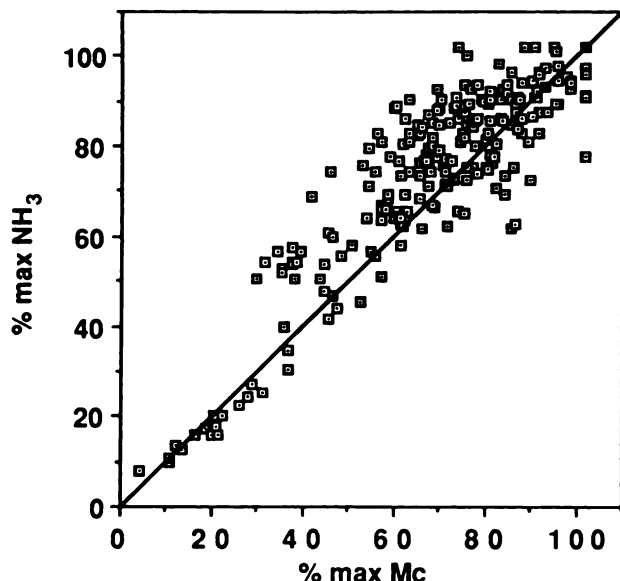


FIGURE 2
Correlation between myocardial ammonia and microspheres uptake both expressed as percent of maximal activity within each tissue slice. The increased spread of the points from the identity line at higher flows is related to the progressive reduction of the ammonia extraction fraction.

$y = 0.97x + 0.68$), both expressed as percentage of maximum.

The in vitro arterial input function curves obtained in the six animals following ammonia injection are shown in Figure 3. It is worth noting that in all dogs the downslope portion of the curve can be fitted by two exponentials with a $t_{1/2}$ of 11.4 ± 4 sec and 34.9 ± 6 sec, respectively. In all cases, arterial ^{13}N activity reached an almost steady level that was only $3.6\% \pm 0.8\%$ of the peak, 180 sec following tracer injection. Comparing each in vitro input function with the corresponding acquired by PET (both expressed as percent of the peak activity; Fig. 4), no significant difference was found with regard to the first downslope part of the curve (where data points were fitted), i.e., before the spillover from tissue activity begins to affect the left ventricular cavity data. Similarly, a good correlation was observed between the integrals of the input function computed from in vitro (exponential fit) and PET (gamma fit) data ($r = 0.93$), after normalization of the two curves on the respective peak activities.

The integrals of the input function for each dog, computed according to the three different approaches, are reported in Table 1. The integral of the curve from 0 to 14 min (total) was 2.1 and 2.6 times greater than the "2-min" and "exponential" integral, respectively. The exponential integral was on average 19% smaller than the 2-min integral. The variation coefficient between the latter two integrals was only 7%. Consequently, according to the RMBFe equation described

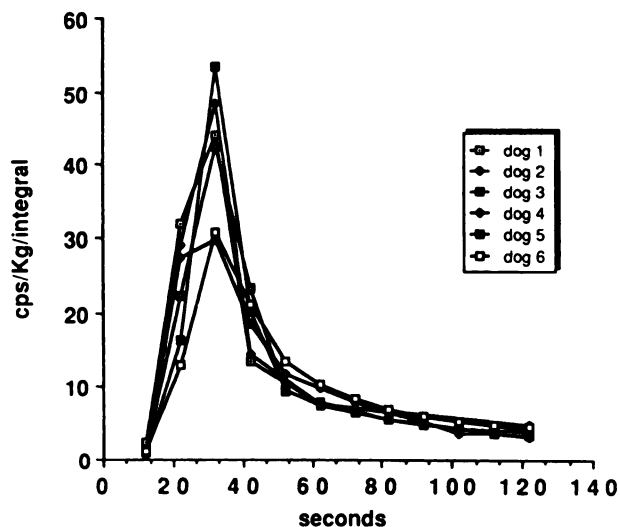
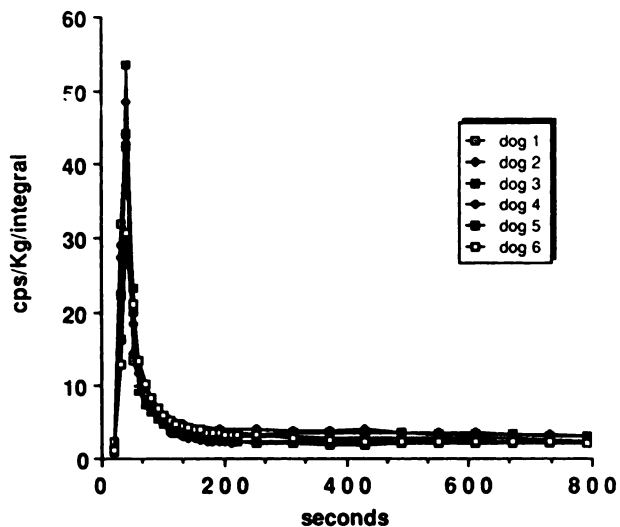


FIGURE 3
Time-activity curves of the six dogs obtained by arterial blood samples measured in the well counter. Activity values are expressed in cts/sec divided by the weight of the tissue sample and normalized for the integral of each curve. In the upper panel data points are plotted from time of injection to the end of the experiments: a steady-state blood activity is reached in all dogs after 200 sec from injection ($\sim 5\%$ of the peak activity). The first 120 sec of the curves are expanded in the lower panel, to show the behavior of the downslope portion: it is very similar for almost all the experiments.

above, the three integration methods provide different relations when compared with microsphere flow.

In the upper panel of Figure 5, the effect of the different integration of the input functions on the in vitro measurements of $^{13}\text{NH}_3$ -RMBF is shown. Data are expressed as RMBF times extraction (RMBFe); epiendocardial values of each wedge are averaged (after weight normalization) and displayed as single points. It is evident that the function calculated using the "exponential" integral approach ($y = 0.12 + 0.85x - 0.08x^2$) best approached the actual microsphere flow (at each flow rates and particularly at higher flows) than the

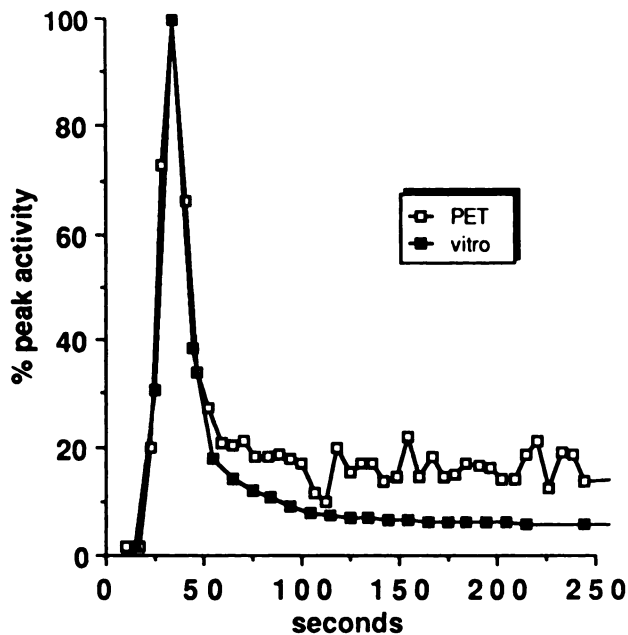


FIGURE 4
Early ammonia activity in blood, assessed both by in vitro and PET measurements, is shown as a function of time (0 = injection time). Data are expressed as percent of peak activity. There is a superimposition of the two curves till the end of their downslope portion when the spillover from tissue activity begins to significantly affect the PET measurements made in the left ventricular cavity.

one using the 2-min approach ($y = 0.16 + 0.63x - 0.06x^2$), while a poor correlation is obtained when the "total" integral is used.

The lower panel of Figure 5 depicts the linear relation between $^{13}\text{NH}_3$ -RMBFe (all epi-endocardial values) and the natural logarithm of microsphere flow, using the "exponential" integral approach. The average percent deviation of the measured points from the linear fit is smaller in comparison with the polynomial fit (15.3% versus 16.2%). We used this kind of relation for the extraction fraction correction of the in vivo data.

The same algorithm for input function computation was used for quantitation of RMBFe by PET. In vivo measurement of RMBFe by $^{13}\text{NH}_3$ and the tomograph was found to correlate well ($r = 0.96$) with the in vitro microsphere values over the flow range of 0.2 to 5 ml/min/g. The polynomial regression curve for all data points was $y = -0.018 + 0.96x - 0.09x^2$ (Fig. 6, upper panel). RMBFe obtained from PET data was corrected for the variable tissue ammonia extraction fraction derived from the relationship between in vitro $^{13}\text{NH}_3$ RMBFe and the log transformed microsphere RMBF. The correlation between actual RMBF assessed with radioactive microspheres and RMBF obtained from $^{13}\text{NH}_3$ and PET after correction for extraction, is shown in the lower panel of Figure 6.

Finally, the time course of myocardial ^{13}N uptake after i.v. injection was investigated by serial scans in order to optimize imaging time. The variation of myocardial ^{13}N content as a function of time in the last five 2-min PET acquisitions (mid-scan values) is shown in Figure 7. It is worth noting that tissue activity increased <8% from the first to the last acquisition and was rather steady from $t = 10$ min to the end of the study. This indirectly indicates that at 4 min after tracer injection most of the in blood ^{13}N activity does no longer belong to $^{13}\text{NH}_3$. The last scan was then used for the computation of RMBFe with PET.

DISCUSSION

In the present study, the concentration of ammonia in blood and myocardial tissue was measured in the same animals both with well counting in vitro and in vivo by means of PET. A good agreement between the two sets of data was found for the blood as well as for the tissue samples. The accuracy and reliability of the quantitative measurements of $^{13}\text{NH}_3$ arterial input function and myocardial uptake by PET have been assessed. The approach used allowed for a step-by-step

TABLE 1
Integrals (Kcts) from the Input Function Curves of the Six Dogs (In Vitro Data)

	Total ¹	2 min ¹	Exp. ²	Total/2 min	Total/Exp.	Exp./2 min
Dog #1	12,509	5,064	3,888	247%	322%	77%
Dog #2	16,982	6,520	4,876	260%	348%	75%
Dog #3	27,112	15,303	12,769	177%	212%	83%
Dog #4	21,740	12,351	10,515	176%	207%	85%
Dog #5	24,708	11,793	9,278	210%	266%	79%
Dog #6	20,022	9,543	8,493	210%	236%	89%
Average	20,512	10,096	8,303	213%	265%	81%
C.V. ³	26%	38%	41%	16%	22%	7%

¹ Integral from 0 to 15 min.

¹ Integral from 0 to 2 min.

² Integral derived from the exponential fit approach.

³ Coefficient of variation: s.d./mean %.

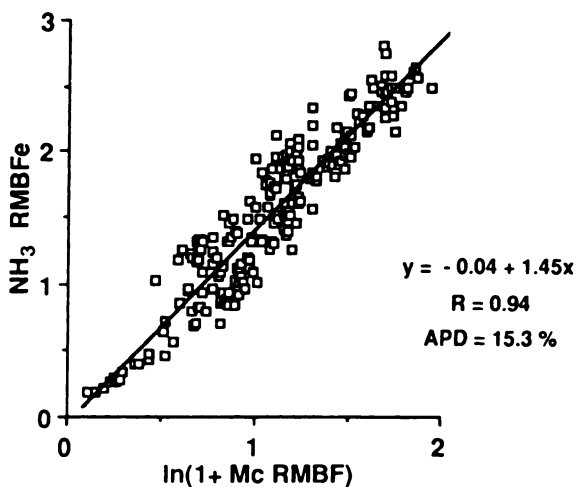
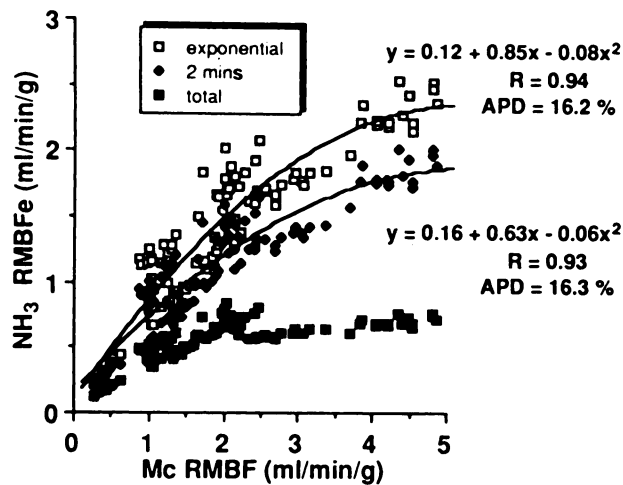


FIGURE 5
(Upper panel) In vitro relationship between regional myocardial blood flow times ammonia extraction (NH_3 RMBFe) and actual flow assessed with microspheres (Mc RMBF) using the three different approaches for calculating the input function integral. A better approximation to actual flow is achieved using the fitted input function (exponential) in comparison to the raw data integral up to 2 min. The use of the total input function in the integral computation, as expected, causes a large underestimation of RMBFe (i.e., too low extraction fraction) and a very poor correlation with actual flow values. For sake of simplicity of this figure, epi-endocardial wedges measurements are represented as an averaged value. APD = average percent deviation of data points from the fitting function. *(Lower panel)* Linear relationship ($R = 0.94$, APD lower than for the polynomial fit) between RMBFe and a log transformation of microsphere data. This relationship can be also expressed as: $\text{RMBF} = e^{(\text{RMBFe} + 0.04)/1.45} - 1$, and thus it can be used for correcting the overall explored flow range for variable ammonia extraction fraction. All values (epicardial and endocardial wedge activities) are represented here.

validation of the biologic parameters involved in calculation of myocardial blood flow by PET.

The results of the present study indicate that, within a wide range of coronary flow values, dynamic PET provides accurate assessment of input function and $^{13}\text{NH}_3$ myocardial concentration which allows for the

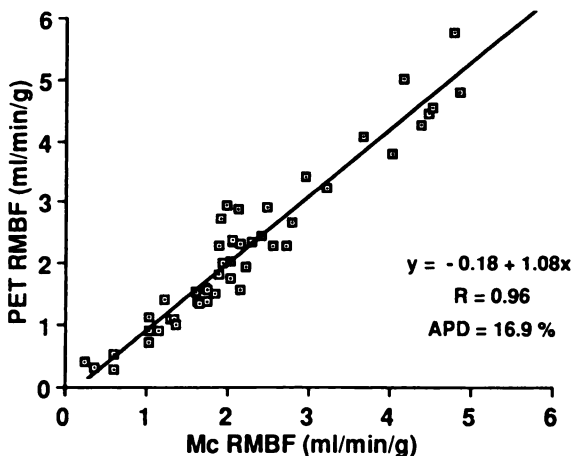
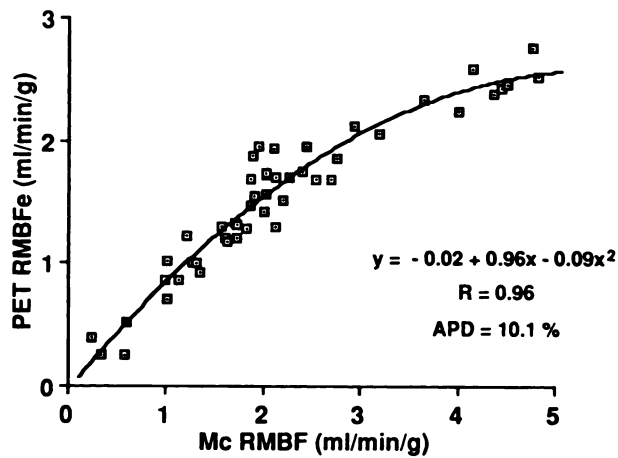


FIGURE 6
(Upper panel) Relationship between $^{13}\text{NH}_3$ regional myocardial blood flow times extraction measured with PET (PET RMBFe) and actual RMBF measured with radioactive microspheres (Mc RMBF). Due to the variable ammonia extraction, data can be fitted with a second degree polynomial function (APD = average percent deviation of data points from the fitting function). *(Lower panel)* A linear relationship was obtained following correction of RMBFe for ammonia extraction using the equation, derived from the in vitro data, which is shown in the lower panel of Figure 5.

computation of RMBF which closely correlates with microsphere flow.

Release of $^{13}\text{NH}_3$ from the myocyte during prolonged, severe ischemia and reperfusion may potentially affect RMBF measurements by this tracer. In order to keep coronary blood flow and hemodynamics almost steady during ^{13}N tissue and blood activity measurements, these clinically applicable situations were not addressed in our study.

The accuracy of the method used for the in vivo evaluation of the variable thickness of the left ventricle could not be assessed, since there was no practical way to make a reference measure. Echo measurement could be of help if obtained simultaneously and if obtained from comparable transaxial slices (goals very difficult to achieve). Post mortem measurements of myocardial

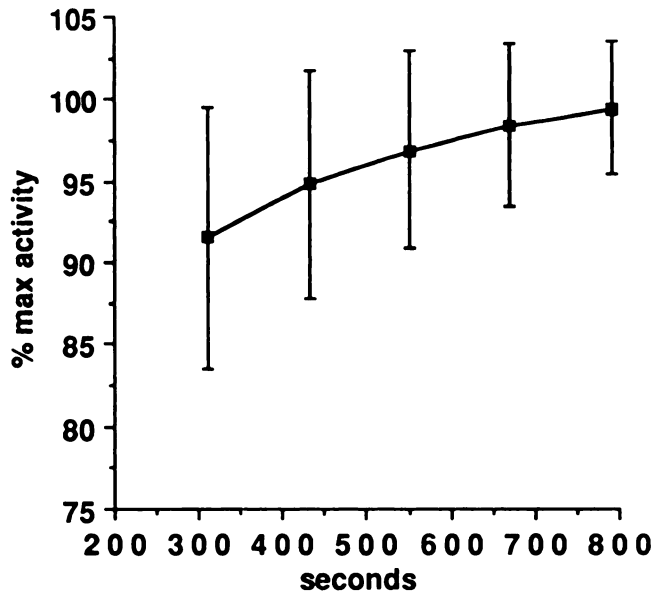


FIGURE 7
Myocardial ammonia uptake from 300 to 840 sec derived from the last five static acquisitions performed by PET. Each point (mean \pm 2 s.d.) is normalized to the relative maximal activity. A significant ($p < 0.001$) but small mean increment ($<7\%$) in ^{13}N activity from the 300-sec scan to the 840-sec scan is observed.

thickness are not representative and reliable, particularly in the ischemic regions. The described approach might probably have some limitations for the ischemic myocardium, for which the same thickness of adjacent non ischemic regions is used, but the precise definition of the wall edges cannot be determined when the count rate is very low. However, the overall correlation between in vitro and in vivo data in our study may represent a good, although indirect, index of accuracy of the correction.

Nitrogen-13-ammonia Blood Clearance and Definition of the Input Function

The $^{13}\text{NH}_3$ kinetics in blood and myocardium have been widely explored and reported in the literature (2-4,6-9). After an i.v. bolus injection, $^{13}\text{NH}_3$ is rapidly cleared from the vascular compartment. Almost all the tracer is metabolically trapped into tissues within the first capillary transits and its release is virtually negligible during the first 2 min of the PET study (9), i.e., in the phase involved in the input function evaluation. A small amount of ^{13}N activity circulates at 3 min after injection ($<5\%$ of the peak value) and is thought to derive mainly from ^{13}N -labeled amino acids (alanine and glutamine) and urea. By the tenth minute after injection, all of the ^{13}N activity is present as an ammonia metabolite (15). When ammonia clearance rate from blood was calculated and plotted as a function of arterial ammonia concentration, a linear relationship

was found (15). These findings indicate that ammonia clearance is a first order process at normal arterial concentrations.

For the above reasons, and because of the consistent behavior of the downslope portion of $^{13}\text{NH}_3$ arterial curves in our study, we used an "exponential" fit of the curve to derive the input function integral. A similar approach (i.e., a gamma variate fit, owing to an increased number of points) could be used with input function curves derived from PET, due to the good correspondence between the in vitro and in vivo downslope part of the curve. The integrals of the input function calculated from PET data closely correlated with those obtained from in vitro measures. The blood samples for in vitro measurements (2 ml each) were taken manually in a very short time and through a catheter of negligible volume compared to the volume of the sample itself. For this reason, a good correlation was found with the PET data without the need of applying a deconvolution; this correction technique, on the contrary, is always required when a low-flow peristaltic pump and a direct continuous monitoring of the activity variations in the tubing are used (16). The "exponential fit" algorithm provided a closer relation between $^{13}\text{NH}_3$ RMBF and actual microsphere flow than that using the 2-min integral (6).

In agreement with previous reports (6), our results confirm that when RMBF is measured with $^{13}\text{NH}_3$ using the "total" input function, i.e., integrating from $t = 0$ (beginning of tracer injection) to the time when tissue activity was measured (i.e., $t = 14$ min), flow values are consistently and markedly underestimated.

RMBF Measurement with $^{13}\text{NH}_3$

Although $^{13}\text{NH}_3$ is used to compute RMBF with PET, there is concern about the systematic underestimation of flow which is known to occur with this tracer. Several mechanisms are known to be responsible for the underestimation. The extraction of ammonia by the myocardium varies inversely with coronary flow (4) and is affected by the metabolic state of the tissue (7,8). While only extreme variations in the metabolic state affect the fate of $^{13}\text{NH}_3$ in the myocardium (4), a more important role is played by the flow dependency of ammonia extraction. Schelbert et al. (4) reported a $^{13}\text{NH}_3$ extraction fraction by the myocardium of nearly 100% at low flows (below 1 ml/min/g) and 82% at control flows. The extraction fraction decreased progressively with increasing flow, approaching 50% for flow rates higher than 3 ml/min/g. Indeed, our data are in agreement with this finding of a significant decrease of ammonia extraction beyond flows of 2.5 ml/min/g (Fig. 5).

In practical terms, RMBF computed without correction for the variable extraction fraction of the tracer will lead to a significant underestimation, particularly at higher flow rates. In the clinical setting, this will not

allow, for instance, the correct assessment of coronary reserve, hampering comparisons of data in transverse and longitudinal studies. Consequently, if one considers the entity of the possible underestimation, in the absence of a correction factor directly derived from human data, it seems conceivable to apply, in clinical studies, the equation derived from the relationship between RMBFe and RMBF in dogs.

As shown in lower panel of Figure 5, a log transformation of the microsphere RMBF was found to have a linear correlation with the ammonia RMBFe. The reasons for choosing this kind of transformation are mainly two. First, the second degree polynomial function used by others (5,6) to correct the full range of ammonia data seems to be rather inadequate. In fact, considering that the equation we used to fit the in vitro data ($y = 0.12 + 0.85x - 0.08x^2$; Fig. 5, upper panel) is a parabolic function with a maximal y of 2.378, any RMBFe measurement assessed with $^{13}\text{NH}_3$ beyond that value would remain uncorrected. The polynomial fit of the relation is shown both in Figure 5 and in Figure 6 only to compare curves with the previous papers. Second, according to the variable ammonia extraction described by the Renkin-Crone Equation 4, the best-fitting function of $^{13}\text{NH}_3$ data would have been the following: $\text{RMBFe} = \text{RMBF} - 0.77 \cdot \text{RMBF} \cdot \text{EXP}(-2.32/\text{RMBF})$. This kind of relationship, however, is not reversible, while the function $\text{RMBFe} = 1.45 \cdot \ln(1 + \text{RMBF}) - 0.04$, is completely superimposable to the previous one in the range 0-5 ml/min/g (differences <2%), and it can also be transformed as $\text{RMBF} = \text{Exp}[(\text{RMBFe} + 0.04)/1.45] - 1$. Therefore, the last equation appears to be the best which can be easily and directly used (with very good approximation) for the correction of variable ammonia extraction on the PET measurements.

An alternative approach for the assessment of RMBF with $^{13}\text{NH}_3$ has been proposed which is based on the correction of arterial ^{13}N activity for ammonia metabolites and the assumption of a three-compartmental model to fit the myocardial and blood time-activity curves (17,18). This method seems to satisfactorily correct for the decreased ammonia extraction at higher flow and to provide a correct estimate of coronary reserve in man. This approach, however, requires the PET measurement of ^{13}N myocardial concentration soon after tracer injection, when the disproportionately higher counts in blood relative to tissue render the spillover of activity important.

In conclusion, the results of the present investigation demonstrate the accuracy and feasibility of noninvasive RMBF measurement with $^{13}\text{NH}_3$ and dynamic PET. Despite the limitations of ammonia as a flow tracer, the method we propose gives RMBF estimates that are very close to actual flow in a wide range of perfusion values.

ACKNOWLEDGMENTS

The authors wish to thank Dr. A. Benassi for the project of the electronic interface of the well counter, Mr. G. Puccini and Mr. A. Riva for their skillful technical assistance.

REFERENCES

1. Phelps ME. Emission computed tomography. *Semin Nucl Med* 1977; 7:337-365.
2. Gould KL, Schelbert HR, Phelps ME, Hoffman EJ. Noninvasive assessment of coronary stenoses with myocardial perfusion imaging during pharmacologic coronary vasodilatation. *Am J Cardiol* 1979; 43:200-207.
3. Schelbert HR, Phelps ME, Hoffman EJ, Huang SC, Selin CE, Kuhl DE. Regional myocardial perfusion assessed with N-13 labeled ammonia and positron emission computerized axial tomography. *Am J Cardiol* 1979; 43:209-218.
4. Schelbert HR, Phelps ME, Huang SC, et al. N-13 ammonia as an indicator of myocardial blood flow. *Circulation* 1981; 63:1259-1272.
5. Nienaber CA, Ratib O, Huang SC, Weinberg I, Phelps ME, Schelbert HR. Quantitative assessment of regional myocardial perfusion using dynamic PET and N-13 ammonia [Abstract]. *J Nucl Med* 1988; 29:782-783.
6. Shah A, Schelbert HR, Schwaiger M, et al. Measurement of regional myocardial blood flow with N-13 ammonia and positron-emission tomography in intact dogs. *J Am Coll Cardiol* 1985; 5:92-100.
7. Krivokapich J, Huang SC, Phelps ME, MacDonald NS, Shine KI. Dependence of $^{13}\text{NH}_3$ myocardial extraction and clearance on flow and metabolism. *Am J Physiol* 1982; 242: H536-542.
8. Bergmann SR, Hack S, Tewson T, Welch MJ, Sobel BE. The dependence of accumulation of $^{13}\text{NH}_3$ by myocardium on metabolic factors and its implication for quantitative assessment of perfusion. *Circulation* 1980; 61:34-43.
9. Rosenspire KC, Schwaiger M, Mangner TJ, et al. Metabolic fate of N-13 ammonia in human blood: implications for quantification of myocardial blood flow by PET [Abstract]. *J Nucl Med* 1988; 29:783-784.
10. Tamaki N, Senda M, Yonekura Y, et al. Dynamic positron computed tomography of the heart with a high sensitivity positron camera and nitrogen-13-ammonia. *J Nucl Med* 1985; 26:567-575.
11. Vaalburg W, Kamphuis JAA, Beerling-van der Molen HB, Reiffers S, Rijkskamp A, Woldring MG. An improved method for the cyclotron production of ^{13}N -labeled ammonia. *Int J Amm Rad Isot* 1975; 26:316-318.
12. Heymann MA, Payne BD, Hoffman JIE, Rudolph AM. Blood flow measurements with radionuclide labeled particles. *Prog Cardiovasc Dis* 1977; 20:55-79.
13. Spinks TJ, Guzzardi R, Bellina CR. Performance characteristic of a whole-body positron tomograph. *J Nucl Med* 1988; 29:1833-1841.
14. Thompson HK, Starmer CF, Whalen RE, McIntosh HD. Indicator transit time considered as a gamma variate. *Circ Res* 1964; 14:502-515.
15. Lockwood AH, McDonald JM, Reiman RE, et al. The dynamics of ammonia metabolism in man: effects of liver disease and hyperammonemia. *J Clin Invest* 1979; 63: 449-460.
16. Weinberg IN, Huang SC, Hoffman EJ, et al. Validation of PET-acquired input functions for cardiac studies. *J Nucl Med* 1988; 29:241-247.

17. Schwaiger M, Hutchins GD, Krivokapich J, Schelbert HR, Rosenspire K, Kuhl DE. Pet assessment of coronary reserve (CR) in humans using a tracer kinetic model for N-13 ammonia [Abstract]. *Circulation* 1988; 78:II-597.
18. Smith GT, Huang SC, Nienaber CA, Krivokapich J, Schelbert HR. Noninvasive quantification of regional myocardial blood flow with N-13 ammonia and dynamic PET [Abstract]. *J Nucl Med* 1988; 29:940.